



Published in final edited form as:

Prostate. 2015 January ; 75(1): 23–32. doi:10.1002/pros.22886.

Resolution of chronic bacterial-induced prostatic inflammation reverses established fibrosis

Letitia Wong^{1,2}, Paul R. Hutson³, and Wade Bushman^{1,*}

¹Department of Urology, University of Wisconsin-Madison, Madison, Wisconsin, USA

²Molecular and Environmental Toxicology Center, University of Wisconsin-Madison, Madison, Wisconsin, USA

³School of Pharmacy, University of Wisconsin-Madison, Madison, Wisconsin, USA

Abstract

Background—Prostatic inflammation has been suggested to contribute to the etiology of lower urinary tract symptoms by inducing fibrosis. We previously used a well-characterized mouse model of bacterial-induced prostate inflammation to demonstrate that chronic prostatic inflammation induces collagen deposition. Here, we examined stability of the newly synthesized collagen in bacterial-induced prostatic inflammation and the reversibility of fibrosis after resolution of infection and inflammation.

Methods—Uropathogenic *E. coli* 1677 was instilled transurethrally into adult C3H/HeOJ male mice to induce chronic prostatic inflammation. Collagen was labeled by ³H-proline administration for 28 days post-inoculation and ³H-hydroxyproline incorporation measured to determine stability of the newly synthesized collagen. Inflammation score was graded using a previously established system and total collagen content was measured by picosirius red staining quantitation and hydroxyproline content. Resolution of inflammation and reversal of collagen deposition was assessed after treatment with antibiotic enrofloxacin for two weeks on day 28 post-inoculation followed by an eight-week recovery period.

Results—Decay analysis of incorporated ³H-hydroxyproline revealed the half-life of newly synthesized collagen to be significantly shorter in infected/inflamed prostates than in controls. Treatment with antibiotic enrofloxacin completely eradicated bacterial infection and allowed resolution of inflammation. This was followed by marked attenuation of collagen content and correlation analysis verified a positive association between the resolution of inflammation and the reversal of collagen deposition.

Conclusions—These data demonstrate, for the first time, that inflammation-induced prostatic fibrosis is a reversible process.

Keywords

Prostate; Reversibility of fibrosis; Resolution of inflammation

*Correspondence to: Dr. Wade Bushman, MD, PhD, Department of Urology, University of Wisconsin-Madison, K6/562 Clinical Sciences Center, 600 Highland Avenue, Madison, WI 53792, USA. bushman@urology.wisc.edu.

Introduction

Prostatic inflammation is frequently present in aging men. It has been suggested to be a major etiological factor for benign prostatic hyperplasia (BPH) and lower urinary tract symptoms (LUTS) as there is accumulating evidence showing that the degree of inflammation was correlated with symptom severity and disease progression of BPH/LUTS [1,2]. However, the underlying mechanism for this association remains to be established. Several studies have shown that prostatic fibrosis is strongly associated with impaired urethral function and LUTS severity [3,4]. This led to the hypothesis that prostatic inflammation contributes to the pathogenesis of BPH/LUTS by inducing prostatic fibrosis and impairing opening of the bladder neck – prostate complex during voiding. Using a previously described mouse model of bacterial-induced prostatic inflammation [5], we recently characterized the fibrotic response to inflammation in the prostate [6]. Our findings demonstrated that chronic prostatic inflammation results in a significant increase in prostate collagen content, strongly supporting a role for inflammation in prostatic fibrosis.

Given that inflammation-induced prostatic fibrosis could be a major contributing factor in the development and progression of BPH/LUTS, it is imperative to determine whether the injured prostate has the capacity to resolve and remodel the established fibrosis induced by inflammation. In this study, we extended our work to investigate the reversibility of fibrosis induced by inflammation. We first measured the stability of the newly synthesized collagen to examine whether collagen induced in prostate inflammation undergoes remodeling and degradation. We then used antibiotic treatment to induce resolution of bacterial-induced inflammation and measured reversal of the associated fibrosis over an eight-week recovery period. Our findings demonstrate, for the first time, that prostatic fibrosis induced by chronic inflammation is at least partly reversible.

Materials and Methods

Transurethral Instillation

Transurethral instillation was performed as previously described [5]. 8-week old C3H/HeOuJ male mice (Jackson Laboratories, Bar Harbor, Maine) were anesthetized with isoflurane and catheterized with a lubricated sterile polyethylene catheter per urethra. Inoculation was performed by a single transurethral instillation of uropathogenic *E. coli* 1677 (2×10^6 CFU/ml) or sterile PBS in a volume of 200 μ l.

Antibiotic Treatment

At day 28 post-instillation some animals were treated with 1ml of 100mg/ml enrofloxacin (Baytril® 100, Bayer Corp., Pittsburgh, PA) per 450 ml drinking water for two weeks. Fresh water with enrofloxacin was replaced every 3-4 days. Other animals received sham treatment (regular drinking water). After two weeks of treatment, all animals received regular drinking water. Animals were sacrificed either immediately or 8 weeks after the end of enrofloxacin/sham treatment. The prostatic lobes (ventral prostate, dorsolateral prostate, anterior prostate) were harvested separately and were used for bacterial culture and histology. The whole mouse prostates were collected and used for hydroxyproline assay and

measuring the incorporation of ^3H -hydroxyproline to determine collagen stability. Four to six mice per treatment group were analyzed for histology. Four mice per treatment group were used for bacterial counts. Four to five mice per treatment group were used for hydroxyproline assay. Three to eight mice per time point per treatment group were used for collagen stability measurement.

Bacterial Counts

Each prostatic lobe was collected separately, weighed and homogenized in 400 μl of sterile cold PBS. The homogenate was serially diluted to 1:100 and 1:1000 and plated onto Levine EMB agar at 37°C for 24 hours. Each dilution was plated in duplicate. Prostatic bacterial titers are presented as the mean colony-forming units (CFUs) $\times 10^3$ /prostate weight (mg) \pm standard error of the mean (SEM).

Quantitation of Inflammatory Degree

Tissues were fixed in 10% formalin, imbedded in paraffin and serially sectioned at 6 μm . Standard H&E staining was performed for histology. Using our previously established scoring system [5], the severity of inflammation was graded in at least 3 random 10 \times fields of H&E sections from each prostatic lobe. Data are presented as the mean inflammation score \pm SEM.

Quantitation of Collagen Content

Picrosirius Red Staining—Adjacent tissues sections of H&E stained slides were used for picrosirius red staining. The staining was performed by incubating slides in 0.1% sirius red in saturated aqueous solution of picric acid for one hour at room temperature. Images were taken by digital camera using NIS Element software under a Nikon Eclipse 80i polarized light microscope. The settings of the software and microscope remained unchanged throughout the observation for the purpose of quantitation and comparisons. The color staining that shows up under polarizing microscope corresponds to the birefringence of collagen fibers [7]. Quantitation of the staining for collagen content was then determined by using NIH Image J. Briefly, the images were converted from RGB to 8-bit gray scale and the intensity of the three color channels was summed into one image. The images were manually thresholded to define the collagen staining and a constant value of the threshold was set for all the images analyzed. The region of interest (prostatic tissues) was manually outlined to analyze the area that was stained for collagen. Large blood vessels and nerve fiber bundles in the prostate were eliminated in the quantitation. Data are presented as the mean percentage of collagen area \pm SEM.

Hydroxyproline Assay for Collagen Content by High-Performance Liquid Chromatography (HPLC)—Mouse prostate tissues were harvested, snap frozen in liquid nitrogen, and stored at -80°C until further analysis. The procedure was performed as previously described with some modifications [8]. The tissues were thawed on ice and weighed. Each tissue sample was homogenized in 2ml of 12N HCl with a motorized homogenizer in a clean glass tube. 75 μl of 20mM sacrosine (reagent grade) as internal standard was mixed in the homogenate. Then, the glass tubes containing the tissue homogenate were tightly capped to prevent evaporation and were incubated in a 110°C

heating block for 18 hours. The hydrolysates were allowed to cool to room temperature, neutralized with 2ml of 12N NaOH and 1ml of borate buffer (0.7M boric acid in water, pH 9.5 with NaOH), and were adjusted to a pH 9.5 with NaOH and HCl. Aliquots of 500 μ l of the sample solution were used for subsequent derivatization process. Some samples were run in duplicate or triplicate for intra-day reaction consistency and these same samples were run on the next day for inter-day reaction consistency. Hydroxyproline (reagent grade) standards of 0.3125, 0.625, 1.25, 2.5, 5, 10, 20mM with 7.5mM L-proline (reagent grade) in water were prepared. 200 μ l of each hydroxyproline standard was mixed with 75 μ l of 20mM sarcosine, 1.8ml of 12N HCl, 2ml of 12N NaOH and 1ml of borate buffer. The solutions were then adjusted to pH 9.5. Aliquots of 500 μ l of the hydroxyproline standard solution were used for subsequent derivatization process.

Aliquots (500 μ l) of tissue homogenate or hydroxyproline standard were added with 700 μ l of borate buffer. The following procedures were performed in dark. The solutions were mixed with 100 μ l of OPA solution (50mg *o*-phthalaldehyde dissolved in 1ml acetonitrile and 26 μ l of reagent grade β -mercaptoethanol) by vortexing and allowed to react at room temperature for 1 minute. The solution was then mixed with 100 μ l of iodoacetamide solution (140mg/ml of iodoacetamide in acetonitrile) by vortexing and reacted at room temperature for 1 minute. 600 μ l of 5mM FMOC-Cl in acetone was subsequently added, mixed by vortexing and reacted at room temperature for 1 minute. The solutions were then washed three times with 3ml of ethyl ether by vortexing for 30 seconds each. The organic layer was discarded each time. 50 μ l of the aqueous phase was injected into the HPLC. A total of 3 injections were run for each reacted sample or standard. Sample injections were made every 25 minutes without an intervening wash. The isocratic mobile phase was prepared by combining 650ml of 3% glacial acetic acid that was adjusted to pH 4.3 with sodium acetate (reagent grade) with 350ml of acetonitrile, followed by vacuum filtration for degassing. All reagents used were ACS or HPLC grade unless stated otherwise.

The HPLC instrumentation and spectrofluorometer was set up as previously described [8]. The HPLC instrumentation included a Shimadzu LC-10AD HPLC pump, SIL-10A auto injector and system controller. A McPherson Model FL-750 spectrofluorometer was used with the high-sensitivity module, an excitation wavelength of 265nm and without an emission cut-off filter. Separation was achieved by using a Lichrosphere 5 RP18e 250 mm \times 4.60 mm, 5 μ m column. The mobile phase was pumped at a constant rate of 0.75ml/min.

The coefficients of variation for intra-day reaction consistency were less than 2.2% and for inter-day reaction consistency were less than 11%. The height ratio of the internal standard (sarcosine) and hydroxyproline peak was calculated for each sample and standard. The exact amount of hydroxyproline standards in μ g injected into the HPLC was determined by calculating the total dilution made from the original concentration prepared. The standard curve of hydroxyproline standards showed linear regression with $R^2 = 0.995$. The amount of hydroxyproline in μ g presented in the prostate samples was calculated from the peak height ratio of hydroxyproline and internal standard peak into the linear regression equation obtained from the hydroxyproline standard curve. Data are presented as mean hydroxyproline (μ g)/prostate weight (mg) \pm SEM.

Collagen Stability Measured by The Incorporation of ^3H -hydroxyproline

Animals instilled transurethrally with either sterile PBS or uropathogenic *E. coli* 1677 were injected intraperitoneally with $15\mu\text{Ci}$ of L-[3,4- ^3H] proline (specific activity 50-60 Ci/mmol, ARC, Inc.) every two days for 28 days. Animals were sacrificed on day 1, 4, 8, 15, 22, 29, 36, 57, 78, 113 after the last injection of ^3H -proline. The whole prostate was harvested, snap frozen in liquid nitrogen and stored at -80°C until further analysis. The extraction procedure of hydroxyproline has previously been described in detail.[9] Briefly, each tissue sample was placed in a clean glass tube, homogenized in 2ml 12N HCl with a motorized homogenizer and was heated at 110°C for 18 hours. The hydrolysates were then allowed to cool to room temperature and neutralized with 2ml of 12N KOH and 1ml of 1M boric acid in water. The samples were then adjusted to pH 8.7 with KOH and HCl. Aliquots of 2ml of the sample solution were used for subsequent reaction. First, each sample was reacted with 4ml of 0.2M chloramine T-solution in methoxyethanol at room temperature for 20 minutes. 2.4ml of 3.6M sodium thiosulfate in water was then added followed by saturation with 1.5g KCl. The solutions were then washed $3\times$ with 9ml of toluene by vigorously shaking for 5 minutes each. Organic layer was discarded each time. The samples were heated in boiling water for 30 minutes and then allowed to cool down on ice for 10 minutes. Then, 7ml of toluene was added into each sample and mixed by vigorously shaking for 10 minutes. The organic layer that contained hydroxyproline was then removed and mixed with 7ml of liquid scintillation cocktail (Fisher, SX25-5) in a 20ml liquid scintillation vial. Counts per minute (cpm) were measured with a Beckman LS 6000TA liquid scintillation counter. Decay curves were graphed individually for saline instilled and *E. coli* infected prostates by fitting a non-linear regression line through individual data points. The non-linear regression equation is $y = y_0/(1 + y_0 k x)$, where y is remaining ^3H -hydroxyproline radioactivity (cpm)/prostate, y_0 and k are fitting parameters, x is time (days). The graphs are plotted as the natural log of cpm versus time after the last injection of ^3H -proline. The half-life ($t_{1/2}$) is calculated using the following equation $t_{1/2} = 1/(y_0 k)$ obtained from the non-linear regression line.

Statistical Analysis

Inflammation score, collagen area, hydroxyproline content per prostate weight were compared between untreated saline instilled, antibiotic treated saline instilled, untreated *E. coli* infected, and antibiotic treated *E. coli* infected animals. ANOVA (analysis of variance) was employed, followed by a Fisher's protected LSD (Least Significant Difference) test for pair-wise comparisons of different groups. Prior to ANOVA, Levene's test was used to verify the homoscedasticity assumption. The relationship between inflammation score and collagen area for each prostatic lobe in different groups of animals was assessed via Spearman's rank correlation. All analysis was conducted using SAS 9.2 (SAS Institute, Cary NC) software. A P-value < 0.05 was considered statistically significant in two-tailed statistical tests.

Study Approval

All animal studies were approved by the Institutional Animal Care and Use Committee at the University of Wisconsin-Madison.

Results

Collagen Stability In Chronic Bacterial-induced Prostatic Inflammation

Our previous work demonstrated that collagen deposition was significantly increased in bacterial-induced prostatic inflammation and this increase was associated with enhanced collagen synthesis as determined by ^3H -hydroxyproline incorporation and mRNA expression of collagen genes [6]. Here, we measured the stability of the newly synthesized collagen in saline and *E. coli* instilled prostates using a direct *in vivo* radiolabeling method. Inbred C3H/HeOuJ mice instilled transurethrally either with sterile saline or *E. coli* were i.p. injected with ^3H -proline every 2 days for 28 days, a timeframe within which collagen synthesis and content were significantly elevated and peaked post-infection [6]. The radioactivity of ^3H -hydroxyproline in the prostates 1, 4, 8, 15, 22, 29, 36, 57, 78, 113 days after the last ^3H -proline labeling was measured and decay curves generated from these data (Figure 1A and B). We noted a greater ^3H -hydroxyproline content in the infected prostates 1 day after the last labeling. This reflects increased *de novo* collagen synthesis in prostatic inflammation as previously demonstrated [6]. A rapid decrease in ^3H -hydroxyproline content was observed in the first 36 days and the level reached a plateau after 57 days in both groups. The decline in total radioactivity with time signifies disappearance of labeled collagen from the prostate. As determined from the decay curves, the half-life of collagen in the saline instilled prostates was 18.6 days whereas the collagen synthesized in the *E. coli* infected prostates had a half-life of 13.7 days. Our findings revealed that the newly synthesized collagen in chronic prostatic inflammation is relatively less stable and tends to undergo rapid degradative remodeling.

Resolution of Chronic Bacterial-Induced Prostatic Inflammation After Antibiotic Treatment

To ascertain the reversibility of fibrosis, we used antibiotic treatment to resolve infection and inflammation and examined the effect on collagen content. Saline instilled and *E. coli* infected mice were treated with or without enrofloxacin for two weeks on day 28 post-inoculation. We first performed bacterial cultures of each individual prostatic lobe to evaluate the effectiveness of the antibiotic treatment (Table I). Significant bacterial infection was present in all three prostatic lobes from sham-treated *E. coli* infected animals whereas no bacteria were cultured from any infected prostatic lobe after treatment with enrofloxacin. Prostatic tissues from saline instilled mice with and without antibiotic treatment were both culture negative. Histopathological analysis was performed in the ventral prostate (VP) (Figure 2A-B, G-H, M), dorsolateral prostate (DLP) (Figure 2C-D, I-J, N), and anterior prostate (AP) (Figure 2E-F, K-L, O) of sham, and enrofloxacin-treated saline instilled and *E. coli* infected animals after a recovery period of 8 weeks. Saline instilled animals with and without antibiotic treatment had no or minimal prostatic inflammation. All three prostatic lobes from sham-treated *E. coli* infected animals showed evidence of widespread severe inflammation whereas enrofloxacin-treated infected prostates exhibited very mild inflammation with a restoration of the normal prostatic ductal architecture similar to saline instilled controls. These findings demonstrate resolution of chronic bacterial-induced prostatic inflammation after complete elimination of infection with antibiotic treatment.

Reversibility of Excess Collagen Deposition Induced in Response to Chronic Bacterial Prostatic Inflammation

Picrosirius red staining for collagen content was performed on adjacent serial tissue sections of the H&E stained slides from saline instilled and *E. coli* infected male mice with and without antibiotic treatment (Figure 3A-L). As shown in Figure 3M-O, quantitation of the staining showed that there was no significant difference in collagen content of any prostatic lobe between saline instilled animals with and without antibiotic treatment, indicating that treatment with enrofloxacin alone had no effect on collagen deposition in the prostate. A significant increase in collagen deposition was observed in all lobes of sham-treated *E. coli* infected animals. In striking contrast, collagen content in all three prostatic lobes from enrofloxacin-treated *E. coli* infected animals decreased to levels comparable to saline instilled controls. To validate the quantitative result of the picrosirius red staining, hydroxyproline content measured by HPLC was performed (Figure 4). In accordance with the picrosirius red staining, a substantial increase in hydroxyproline content was observed in the prostates of sham-treated *E. coli* infected animals. On the other hand, hydroxyproline content in the prostates of enrofloxacin-treated *E. coli* infected animals was significantly decreased. However, unlike the result obtained from the picrosirius red staining, the reduction of hydroxyproline content in the prostates of enrofloxacin-treated infected animals did not completely reach the baseline level.

To evaluate the relationship between inflammation and reversal of fibrosis, we correlated the inflammation score determined from the H&E images with collagen content measured from the adjacent picrosirius red stained sections for the VP (Figure 5A), DLP (Figure 5B), and AP (Figure 5C) of saline instilled and *E. coli* infected mice with and without enrofloxacin treatment. A significant positive correlation between inflammation and collagen deposition was shown in all three prostatic lobes. Taken together, our results suggest that collagen deposition induced by chronic bacterial-induced prostatic inflammation is at least partly reversible after resolution of inflammation.

Discussion

Fibrosis resulting from excessive deposition of collagen is traditionally recognized as a progressive irreversible condition and an end stage of inflammatory diseases; however, there is compelling evidence in both animal and human studies to support that the development of fibrosis could potentially be a reversible process when the underlying cause is removed or suppressed in various tissues, including the liver and kidney [10-17]. Collagen degradation has been suggested to be a key mechanism mediating the recovery process of fibrosis through the enzymatic action of collagenases. Studies of a rodent model of liver inflammation and fibrosis have shown that increased collagen deposition in the liver of rats injected repeatedly with hepatotoxin carbon tetrachloride (CCl₄) was spontaneously regressed to control level and the extracellular matrix was remodeled to restore the tissue architecture over time after termination of the toxin injection [12,13]. The recovery phase of fibrosis in this model was associated with decreased mRNA expression of collagenase inhibitors, increased expression of interstitial collagenase and increased collagenase activity [13,18,19]. Follow-up studies demonstrated that liver fibrosis with an accumulation of

collagenase-resistant type I collagen in CCl₄-treated Col1a1^{tr} mice failed to undergo significant regression and remodeling [20].

Accumulating evidence has suggested that collagen stabilization is the principal mechanism regulating the rate of collagen degradation and thus determines the reversal of fibrosis in pathological conditions [21-25]. The stability of collagen is conferred by the extent of collagen cross-linking [21]. Previous studies of an *in vitro* model system have demonstrated that formation of cross-links in collagen molecules significantly increased the resistance of collagen to collagenase degradation [21]. In support of this, subsequent studies of an *in vivo* model of liver fibrosis have indicated that incomplete resolution of liver fibrosis in rats treated with CCl₄ was accompanied with a substantial amount of matrix crosslinks as compared to the rats undergoing extensive regression of fibrosis [12]. Indeed, the level of cross-links appears to be increased in the livers from patients with irreversible granulomatous liver fibrosis [26,27] and is associated with the degree of reversibility of fibrosis in experimental models [28,29]. Taken together, these studies support the concept that reversibility of fibrosis is determined by the extent of collagen stabilization.

Our data suggests that the stability of newly synthesized collagen was decreased in chronic bacterial prostatic inflammation. Prostatic fibrosis induced by chronic bacterial inflammation is attributed to a significant increase in *de novo* collagen synthesis as determined by the incorporation of ³H-hydroxyproline [6]. Collagen content increases predominantly between 7 and 14 days post-inoculation. At later time points, collagen content remains elevated but collagen turnover appears homeostatic. Decay analysis of incorporated ³H-hydroxyproline showed that this newly synthesized collagen in prostatic inflammation had a relatively short half-life. Considering that the short-lived ³H-hydroxyproline incorporated in collagen predominantly represents those induced at early time points, our study suggests that collagen produced primarily in early stage of chronic prostatic inflammation undergoes rapid remodeling and is more liable to degradation.

We found that collagen content significantly decreased with resolution of chronic prostatic inflammation. Inflammation was completely resolved after eradication of bacterial infection with antibiotic treatment and an eight-week recovery period. Our quantitative studies revealed that resolution of inflammation and restoration of normal ductal architecture in the prostate was accompanied by marked attenuation of collagen content. These findings were in agreement with our decay study of incorporated ³H-hydroxyproline suggesting that collagen synthesized in chronic prostatic inflammation is susceptible to a rapid degradative remodeling. These findings support the conclusion that inflammation-induced prostatic fibrosis is at least partly reversible when the underlying cause is completely treated and sufficient recovery time is allowed.

It is noteworthy that there was a disparity between the results obtained from picosirius red staining and hydroxyproline content for measurement of collagen deposition. Picosirius red staining showed that prostatic fibrosis in antibiotic-treated infected animals was remodeled through the recovery period of 8 weeks to level comparable to saline instilled controls while the reduced hydroxyproline content in these animals was still significantly different from controls. This difference reflects the distinct mechanism of the two quantitative methods.

Sirius red is an elongated dye molecule that attaches parallel to collagen by reacting its sulfonic acid groups with the basic groups of collagen molecules [7]. Such interaction enhances the birefringence of the highly oriented collagen fibers in tissue sections that can easily be identified in polarized light [30]. Conversely, the biochemical analysis of hydroxyproline content is based on the general concept that this amino acid is abundant and almost exclusively found in collagen. Thus one possibility is that proteins other than collagen also contain hydroxyproline. Indeed, hydroxyproline is found in elastin, hypoxia inducible factor α , complement protein C1q and other non-collagen proteins with collagenous domains [31]. However, the amount of hydroxyproline in these proteins is much less than that in collagen and thus is likely negligible in collagen-enriched tissues [32]. Another explanation is the presence of collagen fragments by MMP cleavage remaining before complete degradation in the antibiotic-treated infected prostates. Collagen fragments lacks the highly-ordered molecular orientation as found in intact collagen fibers and is expected to lose the birefringence promoted by Sirius red staining, while hydroxyproline content in collagen fragments can still be detectable. In support of this, previous studies have demonstrated that a pathological condition characterized by collagen degradation resulted in fragmented and damaged collagens that were weakly birefringent when detected by the picrosirius-polarization method [33].

Prostatic inflammation-induced fibrosis has gained increasing attention as a major contributing factor in the pathogenesis of BPH/LUTS. Several epidemiological studies of human BPH/LUTS have provided evidence for the contribution of excessive collagen deposition and fibrosis in the prostate to impaired urethral function and LUTS. Bercovich and colleagues were the first to report an inverse correlation of uroflow with prostatic fibrosis and symptom score in BPH/LUTS patients [34]. A subsequent study by Ma et al. has demonstrated that prostatic tissues from men with moderate/severe LUTS had a greater mechanical stiffness and a significantly higher collagen content than men with no/mild LUTS [3]. Further, Cantiello et al. have shown that collagen content was significantly higher in prostatic tissues with inflammation than those without inflammation [4]. There were also positive correlations between LUTS severity, inflammation degree, and collagen content. Together, these observational analyses lead to the hypothesis that prostatic fibrosis caused by inflammation increases tissue stiffness that compromises the opening of bladder neck – prostate complex during micturition, and subsequently promotes LUTS. Our recent study of a mouse model of bacterial-induced prostatic inflammation supports this speculation, suggesting a role of chronic inflammation in promoting excessive collagen deposition in the prostate [6]. Therefore, considering that prostatic fibrosis is induced by inflammation and is a potential etiologic factor of BPH/LUTS, it is critical to understand whether the injured/ inflamed prostate has the capacity for recovery from the associated established fibrosis. However, the reversibility of fibrosis has never been examined in the prostate. Our present study is the first report demonstrating that collagen induced in chronic prostatic inflammation is more susceptible to degradation and is at least partly reversible when the underlying cause is resolved.

Conclusions

Collagen deposition induced by chronic prostatic inflammation exhibits a relatively short half-life as compared to the collagen content of the uninflamed prostate. Our findings show that inflammation-induced prostatic fibrosis is at least partly reversible and suggest that fibrosis of the human prostate may be addressed therapeutically by removing the cause of inflammation or suppressing the inflammatory response.

Acknowledgments

This work was supported by NIH R01DK0757, T32 ES007015 from the National Institute of Environmental Health Sciences (NIEHS), NIH, and Herman I. Shapiro Distinguished Graduate Fellowship from UW-Madison School of Medicine and Public Health. Its contents are solely the responsibility of the authors and do not necessarily represent the official views of the funders. The authors also greatly thank Dr. William Ricke's laboratory (UW-Madison) for providing polarizing microscopy and Chee Paul Lin (UW-Madison) for providing statistical analysis.

Grant Sponsors: National Institutes of Health; Grant number: R01DK0757; National Institute of Environmental Health Sciences; Grant number: T32 ES007015

References

1. Robert G, Descazeaud A, Nicolaiew N, Terry S, Sirab N, Vacherot F, Maille P, Allory Y, de la Taille A. Inflammation in benign prostatic hyperplasia: a 282 patients' immunohistochemical analysis. *The Prostate*. 2009; 69(16):1774–1780. [PubMed: 19670242]
2. Nickel JC, Roehrborn CG, O'Leary MP, Bostwick DG, Somerville MC, Rittmaster RS. The relationship between prostate inflammation and lower urinary tract symptoms: examination of baseline data from the REDUCE trial. *European urology*. 2008; 54(6):1379–1384. [PubMed: 18036719]
3. Ma J, Gharaee-Kermani M, Kunju L, Hollingsworth JM, Adler J, Arruda EM, Macoska JA. Prostatic fibrosis is associated with lower urinary tract symptoms. *The Journal of urology*. 2012; 188(4):1375–1381. [PubMed: 22906651]
4. Cantiello F, Cicione A, Salonia A, Autorino R, Tucci L, Madeo I, Damiano R. Periurethral fibrosis secondary to prostatic inflammation causing lower urinary tract symptoms: a prospective cohort study. *Urology*. 2013; 81(5):1018–1023. [PubMed: 23608423]
5. Boehm BJ, Colopy SA, Jerde TJ, Loftus CJ, Bushman W. Acute bacterial inflammation of the mouse prostate. *The Prostate*. 2012; 72(3):307–317. [PubMed: 21681776]
6. Wong L, Hutson PR, Bushman W. Prostatic Inflammation Induces Fibrosis in a Mouse Model of Chronic Bacterial Infection. *PloS one*. 2014; 9(6):e100770. [PubMed: 24950301]
7. Junqueira LC, Bignolas G, Brentani RR. Picrosirius staining plus polarization microscopy, a specific method for collagen detection in tissue sections. *The Histochemical journal*. 1979; 11(4):447–455. [PubMed: 91593]
8. Hutson PR, Crawford ME, Sorkness RL. Liquid chromatographic determination of hydroxyproline in tissue samples. *Journal of chromatography B, Analytical technologies in the biomedical and life sciences*. 2003; 791(1-2):427–430.
9. McNulty RJ. Methods for measuring hydroxyproline and estimating in vivo rates of collagen synthesis and degradation. *Methods in molecular medicine*. 2005; 117:189–207. [PubMed: 16118453]
10. Sohrabpour AA, Mohamadnejad M, Malekzadeh R. Review article: the reversibility of cirrhosis. *Alimentary pharmacology & therapeutics*. 2012; 36(9):824–832. [PubMed: 22966946]
11. Pol S, Carnot F, Nalpas B, Lagneau JL, Fontaine H, Serpaggi J, Serfaty L, Bedossa P, Brechot C. Reversibility of hepatitis C virus-related cirrhosis. *Human pathology*. 2004; 35(1):107–112. [PubMed: 14745732]
12. Issa R, Zhou X, Constandinou CM, Fallowfield J, Millward-Sadler H, Gaca MD, Sands E, Suliman I, Trim N, Knorr A, Arthur MJ, Benyon RC, Iredale JP. Spontaneous recovery from micronodular

cirrhosis: evidence for incomplete resolution associated with matrix cross-linking. *Gastroenterology*. 2004; 126(7):1795–1808. [PubMed: 15188175]

13. Iredale JP, Benyon RC, Pickering J, McCullen M, Northrop M, Pawley S, Hovell C, Arthur MJ. Mechanisms of spontaneous resolution of rat liver fibrosis. Hepatic stellate cell apoptosis and reduced hepatic expression of metalloproteinase inhibitors. *The Journal of clinical investigation*. 1998; 102(3):538–549. [PubMed: 9691091]
14. Chatziantoniou C, Dussaule JC. Is kidney injury a reversible process? Current opinion in nephrology and hypertension. 2008; 17(1):76–81. [PubMed: 18090674]
15. Zeisberg M, Kalluri R. Reversal of experimental renal fibrosis by BMP7 provides insights into novel therapeutic strategies for chronic kidney disease. *Pediatric nephrology*. 2008; 23(9):1395–1398. [PubMed: 18446379]
16. Adamczak M, Gross ML, Krtil J, Koch A, Tyralla K, Amann K, Ritz E. Reversal of glomerulosclerosis after high-dose enalapril treatment in subtotaly nephrectomized rats. *Journal of the American Society of Nephrology : JASN*. 2003; 14(11):2833–2842. [PubMed: 14569093]
17. Boffa JJ, Lu Y, Placier S, Stefanski A, Dussaule JC, Chatziantoniou C. Regression of renal vascular and glomerular fibrosis: role of angiotensin II receptor antagonism and matrix metalloproteinases. *Journal of the American Society of Nephrology : JASN*. 2003; 14(5):1132–1144. [PubMed: 12707384]
18. Fallowfield JA, Mizuno M, Kendall TJ, Constandinou CM, Benyon RC, Duffield JS, Iredale JP. Scar-associated macrophages are a major source of hepatic matrix metalloproteinase-13 and facilitate the resolution of murine hepatic fibrosis. *Journal of immunology*. 2007; 178(8):5288–5295.
19. Watanabe T, Niioka M, Hozawa S, Kameyama K, Hayashi T, Arai M, Ishikawa A, Maruyama K, Okazaki I. Gene expression of interstitial collagenase in both progressive and recovery phase of rat liver fibrosis induced by carbon tetrachloride. *Journal of hepatology*. 2000; 33(2):224–235. [PubMed: 10952240]
20. Issa R, Zhou X, Trim N, Millward-Sadler H, Krane S, Benyon C, Iredale J. Mutation in collagen-1 that confers resistance to the action of collagenase results in failure of recovery from CCl4-induced liver fibrosis, persistence of activated hepatic stellate cells, and diminished hepatocyte regeneration. *FASEB journal : official publication of the Federation of American Societies for Experimental Biology*. 2003; 17(1):47–49. [PubMed: 12475903]
21. Vater CA, Harris ED Jr, Siegel RC. Native cross-links in collagen fibrils induce resistance to human synovial collagenase. *The Biochemical journal*. 1979; 181(3):639–645. [PubMed: 42386]
22. Harris ED Jr, Farrell ME. Resistance to collagenase: a characteristic of collagen fibrils cross-linked by formaldehyde. *Biochimica et biophysica acta*. 1972; 278(1):133–141. [PubMed: 4341725]
23. Harris ED Jr, McCroskery PA. The influence of temperature and fibril stability on degradation of cartilage collagen by rheumatoid synovial collagenase. *The New England journal of medicine*. 1974; 290(1):1–6. [PubMed: 4357162]
24. Hamlin CR, Kohn RR. Evidence for progressive, age-related structural changes in post-mature human collagen. *Biochimica et biophysica acta*. 1971; 236(2):458–467. [PubMed: 4328109]
25. Hamlin CR, Luschin JH, Kohn RR. Partial characterization of the age-related stabilizing factor of post-mature human collagen-I. By the use of bacterial collagenase. *Experimental gerontology*. 1978; 13(6):403–414. [PubMed: 33059]
26. Ricard-Blum S, Bresson-Hadni S, Guerret S, Grenard P, Volle PJ, Risteli L, Grimaud JA, Vuitton DA. Mechanism of collagen network stabilization in human irreversible granulomatous liver fibrosis. *Gastroenterology*. 1996; 111(1):172–182. [PubMed: 8698196]
27. Ricard-Blum S, Bresson-Hadni S, Vuitton DA, Ville G, Grimaud JA. Hydroxypyridinium collagen cross-links in human liver fibrosis: study of alveolar echinococcosis. *Hepatology*. 1992; 15(4):599–602. [PubMed: 1312984]
28. Ricard-Blum S, Liance M, Houin R, Grimaud JA, Vuitton DA. Covalent cross-linking of liver collagen by pyridinoline increases in the course of experimental alveolar echinococcosis. *Parasite*. 1995; 2(2):113–118. [PubMed: 7582375]

29. Ricard-Blum S, Ville G, Grimaud JA. Pyridinoline, a mature collagen cross-link, in fibrotic livers from *Schistosoma mansoni*-infected mice. *The American journal of tropical medicine and hygiene*. 1992; 47(6):816–820. [PubMed: 1471740]
30. Puchtler H, Waldrop FS, Valentine LS. Polarization microscopic studies of connective tissue stained with picro-sirius red FBA. *Beitrage zur Pathologie*. 1973; 150(2):174–187. [PubMed: 4129194]
31. Gorres KL, Raines RT. Prolyl 4-hydroxylase. *Critical reviews in biochemistry and molecular biology*. 2010; 45(2):106–124. [PubMed: 20199358]
32. Edwards CA, O'Brien WD Jr. Modified assay for determination of hydroxyproline in a tissue hydrolyzate. *Clinica chimica acta; international journal of clinical chemistry*. 1980; 104(2):161–167.
33. Borges LF, Gutierrez PS, Marana HR, Taboga SR. Picrosirius-polarization staining method as an efficient histopathological tool for collagenolysis detection in vesical prolapse lesions. *Micron*. 2007; 38(6):580–583. [PubMed: 17126553]
34. Bercovich E, Barabino G, Pirozzi-Farina F, Deriu M. A multivariate analysis of lower urinary tract ageing and urinary symptoms: the role of fibrosis. *Archivio italiano di urologia, andrologia : organo ufficiale [di] Societa italiana di ecografia urologica e nefrologica/Associazione ricerche in urologia*. 1999; 71(5):287–292.

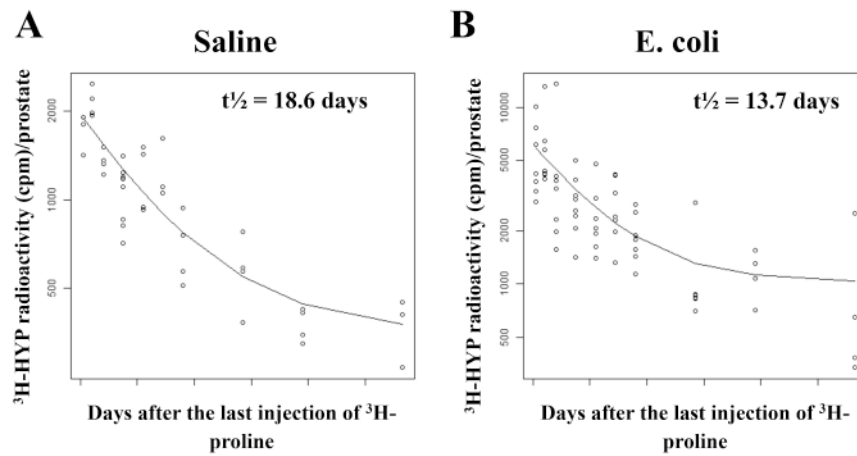


Figure 1.

Decay curves of ^3H -hydroxyproline radioactivity for collagen stability in the prostates of saline instilled (A) and *E. coli* infected (B) mice ($n = 3-8$ per treatment per time point). Each data point represents an individual mouse and the line on each graph represents the nonlinear regression line calculated through the data points. The graphs are plotted as the natural log of cpm/prostate versus time after the last injection of ^3H -proline. Hydroxyproline (HYP); Count per minute (cpm); Half-life ($t_{1/2}$).

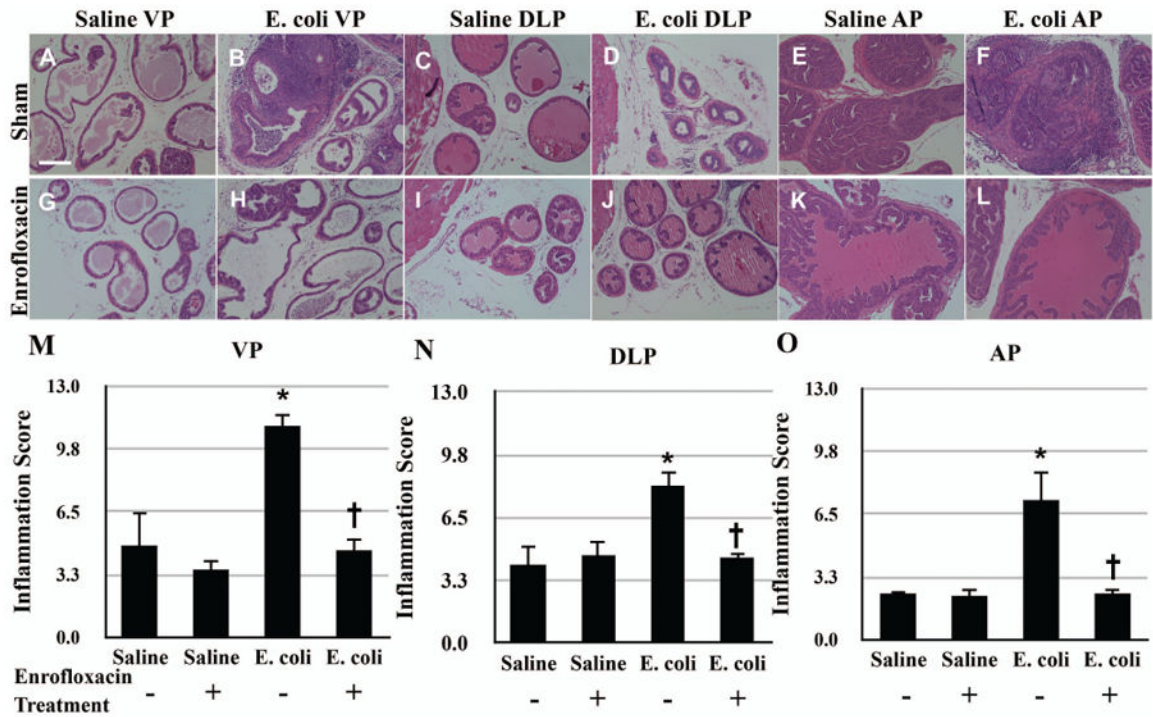


Figure 2.

Representative H&E images of the VP (A-B, G-H), DLP (C-D, I-J), and AP (E-F, K-L) from saline instilled and *E. coli* infected mice 28 days post-instillation that were treated either with enrofloxacin or sham for another 2 weeks. Scale bar 200 μ m in panel A.

Comparisons of the degree of inflammation in the VP (M), DLP (N) and AP (O) from saline instilled and *E. coli* infected mice 28 days post-instillation that were treated either with enrofloxacin or sham for another 2 weeks. The animals were harvested 8 weeks after the antibiotic treatment (n = 4-6 per treatment). Data are presented as mean inflammation score \pm SEM. * indicates a P-value < 0.05 compared to saline treated with sham. † indicates a P-value < 0.05 for *E. coli* treated with enrofloxacin compared to *E. coli* treated with sham. Ventral prostate (VP); Dorsolateral prostate (DLP); Anterior prostate (AP).

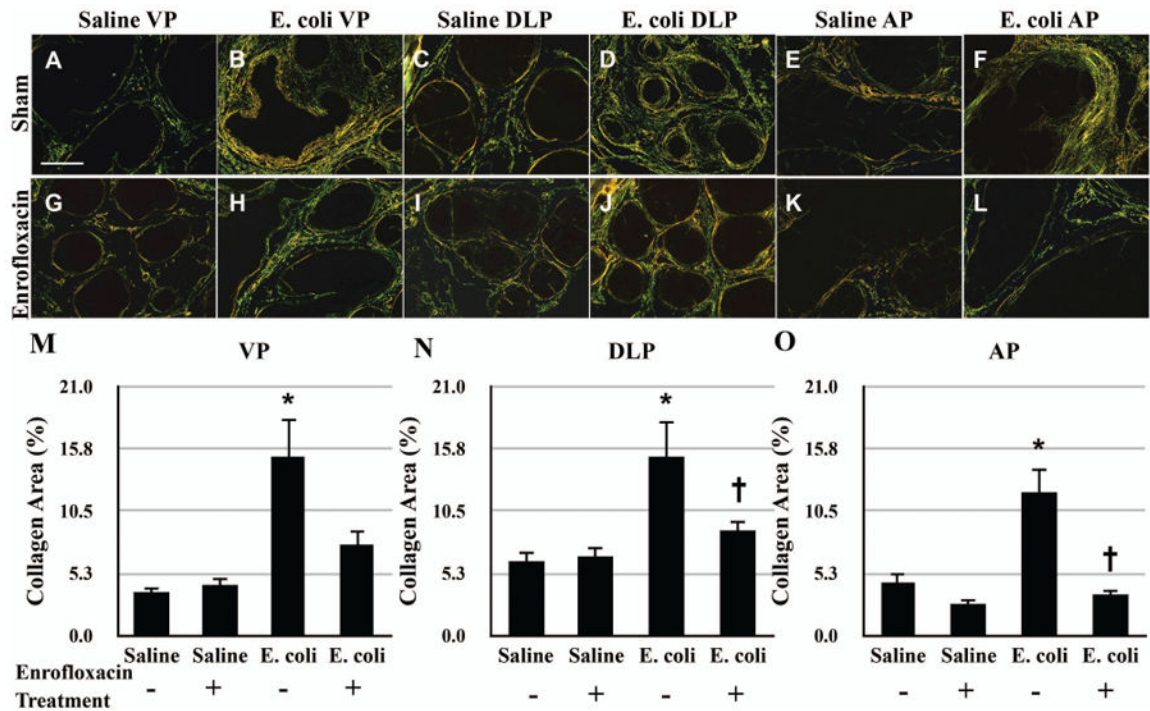


Figure 3.

Representative picrosirius red stained sections of the VP (A-B, G-H), DLP (C-D, I-J), and AP (E-F, K-L) from saline instilled and *E. coli* infected mice 28 days post-instillation that were treated either with enrofloxacin or sham for another 2 weeks. Scale bar 200 μ m in panel A. Comparisons of the collagen content determined by the percentage of picrosirius red stained area in the VP (M), DLP (N) and AP (O) from saline instilled and *E. coli* infected mice 28 days post-instillation that were treated either with enrofloxacin or sham for another 2 weeks. The animals were harvested 8 weeks after the antibiotic treatment (n = 4-6 per treatment). Data are presented as mean percentage of collagen area \pm SEM. * indicates a P-value < 0.05 compared to saline treated with sham. † indicates a P-value < 0.05 for *E. coli* treated with enrofloxacin compared to *E. coli* treated with sham. Ventral prostate (VP); Dorsolateral prostate (DLP); Anterior prostate (AP).

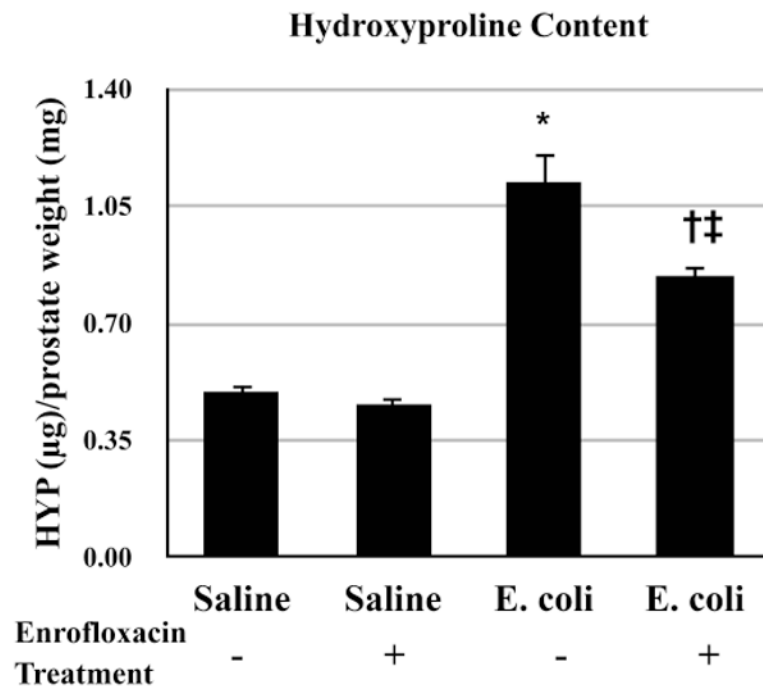
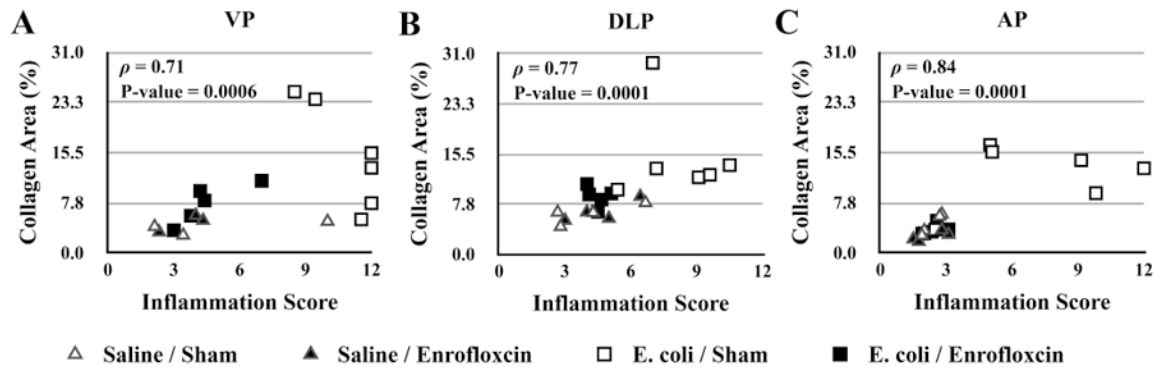


Figure 4.

Comparisons of hydroxyproline content in the prostates of saline instilled and *E. coli* infected mice 28 days post-instillation that were treated either with enrofloxacin or sham for another 2 weeks. The animals were harvested 8 weeks after the antibiotic treatment ($n = 4-5$ per treatment). Data are presented as mean hydroxyproline (μg)/prostate weight (mg) \pm SEM. * indicates a P-value < 0.05 compared to saline treated with sham. † indicates a P-value < 0.05 for *E. coli* treated with enrofloxacin compared to *E. coli* treated with sham. ‡ indicates a P-value < 0.05 compared to saline treated with enrofloxacin. Hydroxyproline (HYP).

**Figure 5.**

Spearman correlation analysis of the relationship between prostatic inflammation and collagen deposition in the VP (A), DLP (B), and AP (C) from saline instilled and *E. coli* infected mice 28 days post-instillation that were treated either with enrofloxacin or sham for another 2 weeks. The animals were harvested 8 weeks after the antibiotic treatment (n = 4-6 per treatment). Ventral prostate (VP); Dorsolateral prostate (DLP); Anterior prostate (AP), Spearman's rank correlation coefficient (ρ).

Table I

Bacterial titers of the prostatic lobes from saline instilled and *E.coli* infected C3H/HeOuJ male mice 28 days post-instillation after enrofloxacin or sham treatment for another 2 weeks (n = 4 per treatment).

CFUs $\times 10^3$ /mg tissue \pm SEM	VP	DLP	AP
Saline Sham	0	0	0
Saline Enrofloxacin	0	0	0
<i>E. coli</i> Sham	21.33(\pm 12.35)	50.26(\pm 34.73)	40.36(\pm 6.65)
<i>E. coli</i> Enrofloxacin	0	0	0

Abbreviations: CFUs Colony forming units; VP Ventral prostate; DLP Dorsolateral prostate; AP Anterior prostate.